Supporting Information

Nickel-vanadium-cobalt ternary layered double hydroxide for efficient electrocatalytic upgrade 5-hydroxymethylfurfural to 2,5-furancarboxylic acid at low potential

Lifang Gao,[a] Xin Wen,[a] Shipeng Liu,[a] Dongyang Qu,[a,b] Yingming Ma,[a] Jianhui Feng[a], Zhiwei Zhong[a], Hongyu Guan*[a] and Li Niu*[a]

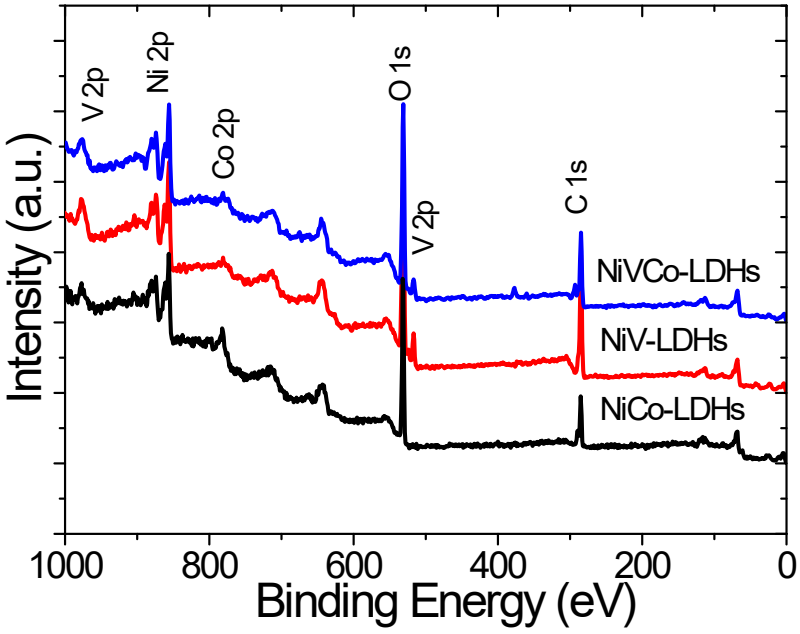

Figure S1. (a) Survey XPS spectra of NiVCo-LDHs, NiV-LDHs and NiCo-LDHs.

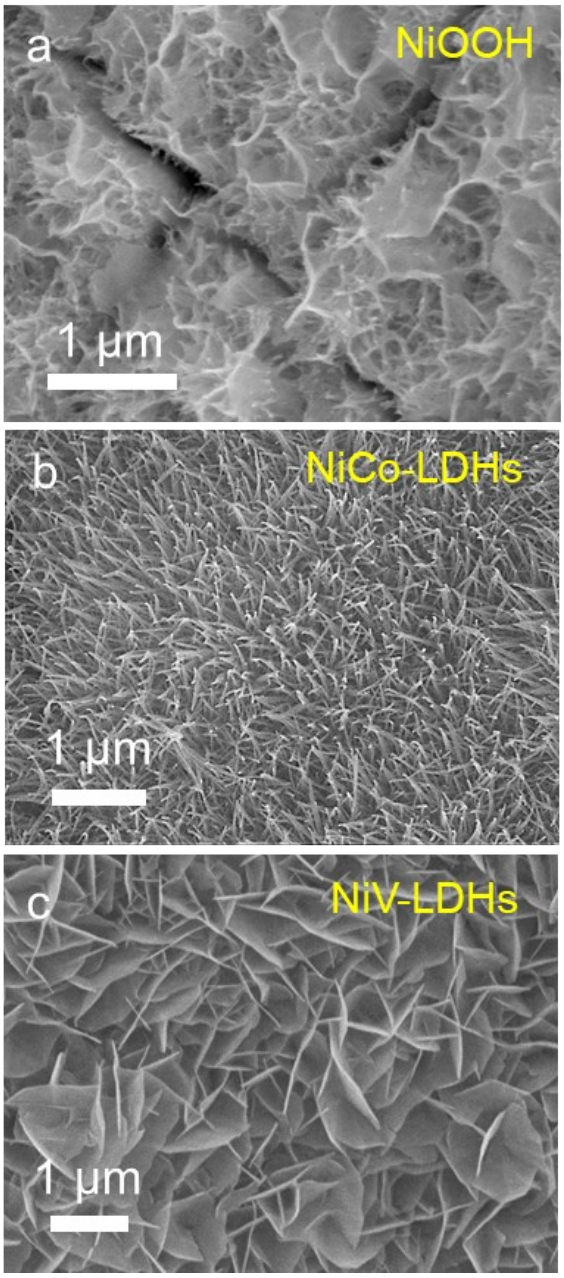

Figure S2. SEM images (a) NiOOH, (b) NiCo-LDHs and (c) NiV-LDHs.

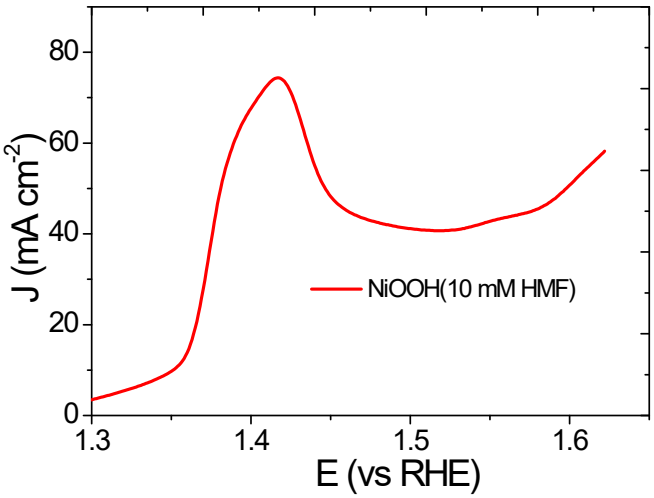

Figure S3 (a) LSV curves of NiOOH at scam rate of 10 mV s^{-1} in 1M KOH with and without 10 mM HMF.

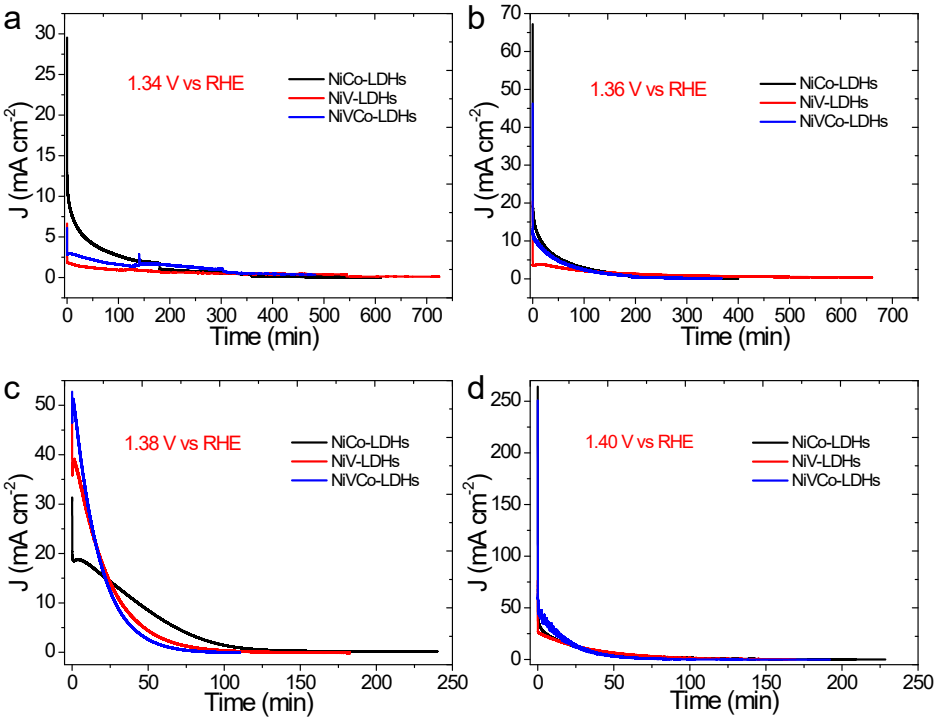

Figure S4 The J-t plots of NiVCo-LDHs, NiV-LDHs and NiCo-LDHs catalysts at electrolysis potential of 1.34 V vs RHE, 1.36 V vs RHE, 1.38 V vs RHE and 1.40 V vs RHE in 1 M KOH with the presence of 10 mM HMF.

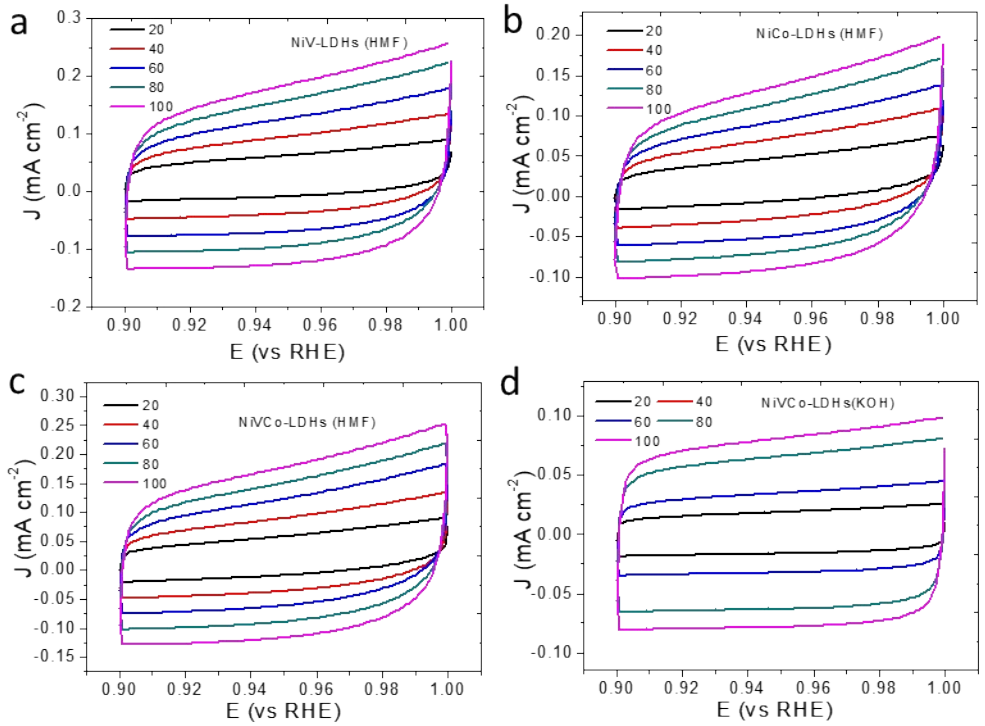

Figure S5. CVs of (a) NiV-LDHs and (b) NiCo-LDHs (c) NiVCo-LDHs with HMF and (b) NiVCo-LDHs without HMF in the non-faradaic capacitance current range at scan rates of 20-100 mV/s.

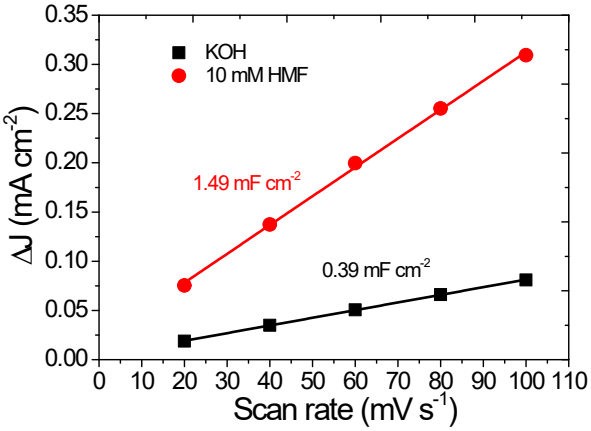

Figure S6. Change of capacitive current density plotted against the scan rate at 0.95 V vs RHE for NiVCo-LDHs with and without HMF.

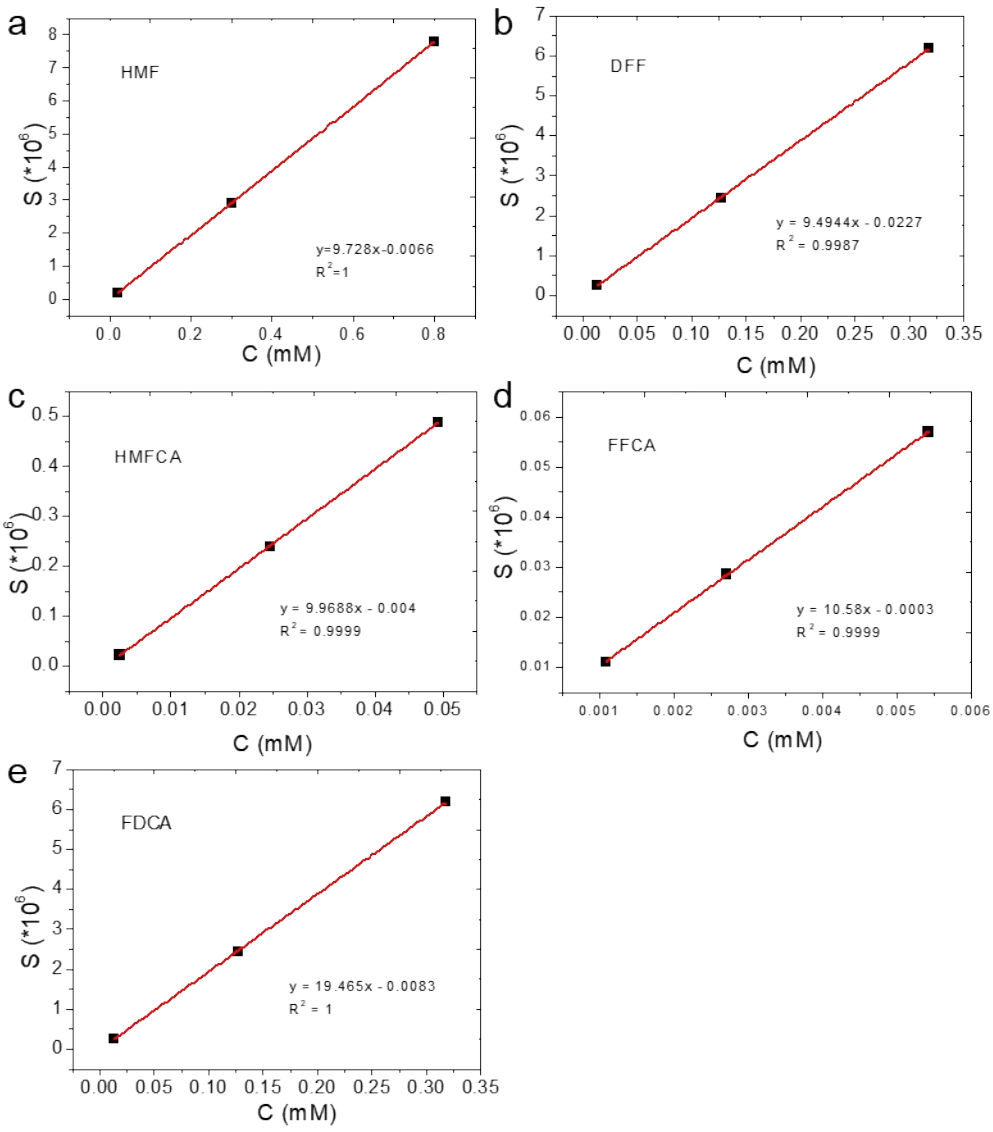

Figure S7. Calibration curves of (a) HMF, (b) DFF, (c) HMFCA, (d) FFCA, and (e) FDCA standard samples.

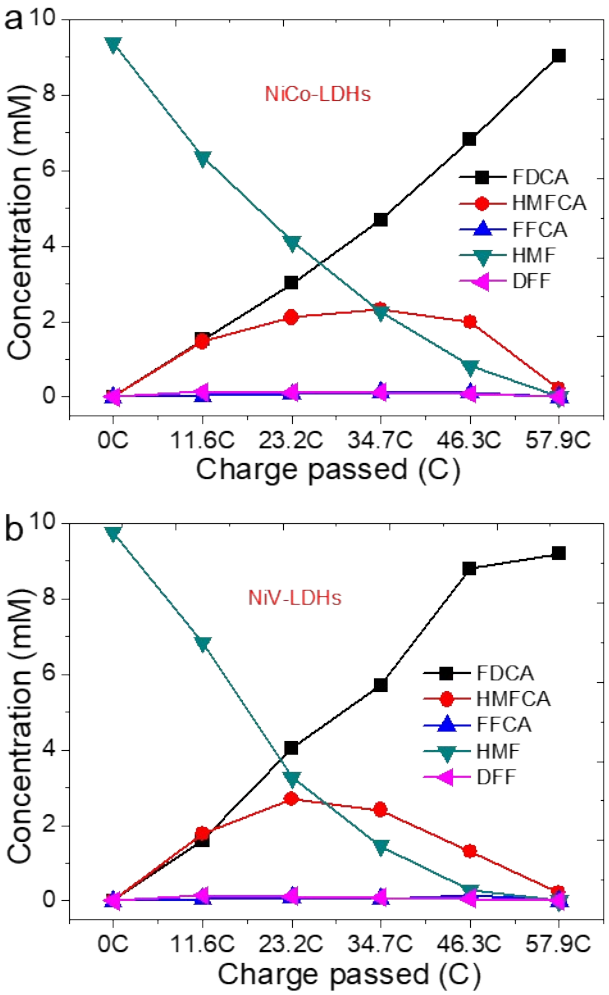

Figure S8. Concentrations change of HMF and its oxidation products with the passed charge at 1.376 V vs RHE in 10 mL 1.0 M KOH containing 10 mM HMF of (a) NiCo-LDHs and (b) NiV-LDHs.

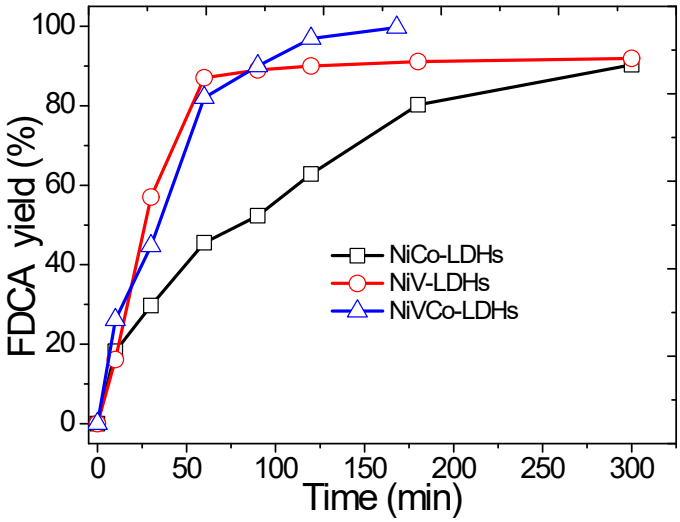

Figure S9 The comparison of FDCA formation rate of NiVCo-LDHs, NiV-LDHs and NiCo-LDHs at 1.376V vs RHE.

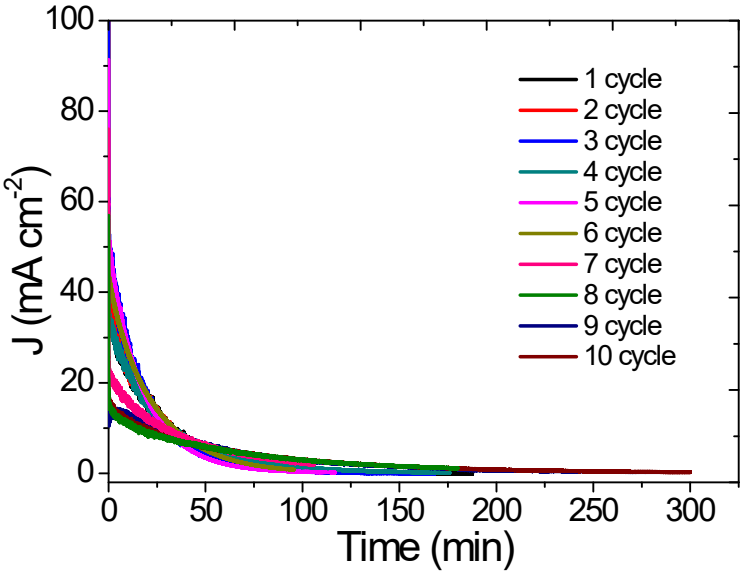

Figure S10 The J-t plots during 10 consecutive cycling electrolysis at 1.376 V vs RHE in 1 M KOH with the presence of 10 mM HMF.

Table S1. Comparison of catalytic performance and cycle stability of the NiVCo-LDHs with other reported catalysts toward HMF electrocatalytic oxidation in alkaline medium.

Catalyst	Benchmark potential (100 mA cm^{-2})	Oxidation potential (vs RHE)	Cycles	FDCA yield	FDCA FE	Reference
NiVCo-LDHs	1.37 V	1.376 V	10	93.2-99.7%	86.5-97.8%	This work
CoAl-LDH	1.59 V	1.52 V	7		95%	1
cationic defect-rich NiFe LDH	>1.70 V	1.48 V	10	96.8%	84.47%	2
NiCoMn-LDHs	>1.60 V	1.50 V （= 35 ℃）	1	91.7%	~65%	3
NiCoFe-LDHs	>1.70 V		1	84.9%	~90	4
$Ni_{0.9}Cu_{0.1}(OH)_2$	>1.70 V	1.45 V	1	91.2%		5
NiO-CMK-1	>2.20 V	1.73 V	5	>80%	NiO-CMK-1	6

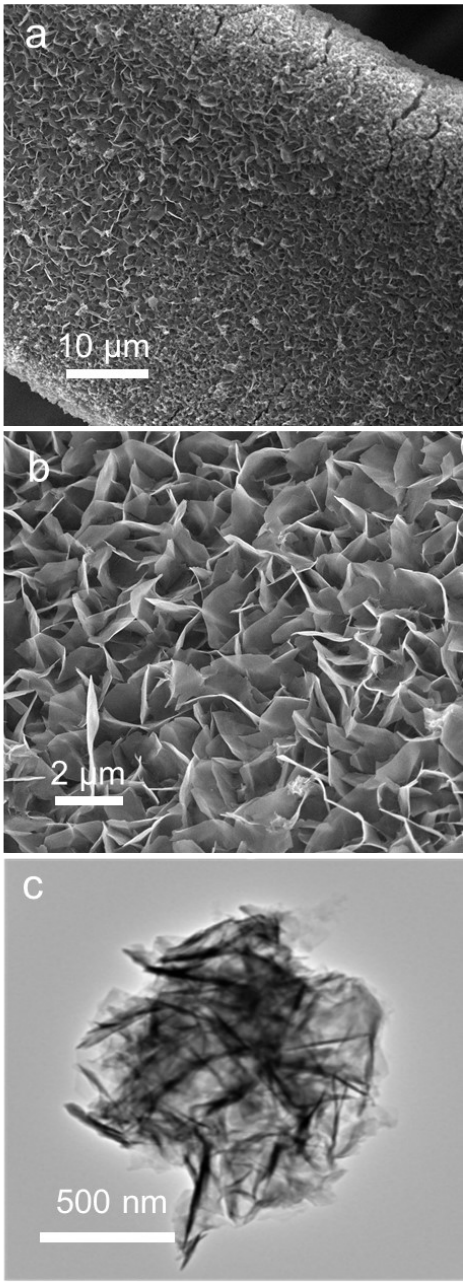

Figure S11 (a) SEM images in low and (b) high-magnification, and (c) TEM image of NiVCo-LDHs after ten successive electrolysis.

Table S2. The comparison of Ni 2p， Co 2p, V 2p and O 1s spectra of fresh NiVCo-LDHs and the post-NiVCo-LDHs sample.

Ni 2p	**Ni $2p_{3/2}$ (eV)**	**Ni $2p_{1/2}$ (eV)**
fresh	854.4	872.3
10 cycles	856.1	873.7

Co 2p	**Co $2p_{3/2}$ (eV)**	**Co $2p_{1/2}$ (eV)**
fresh	780.6	796.2
10 cycles	781.2	796.4

V 2p	**V^{3+}(eV)**	**V^{4+}(eV)**	**V^{5+}(eV)**
fresh	516.2	517.1	518.0
10 cycles	0.0	0.0	0.0

O 1s	**O1(eV)**	**O2(eV)**	**O3(eV)**	**O4(eV)**
fresh	530.7	531.4	532.5	-
10 cycles	530.8	531.5	532.2	533.5

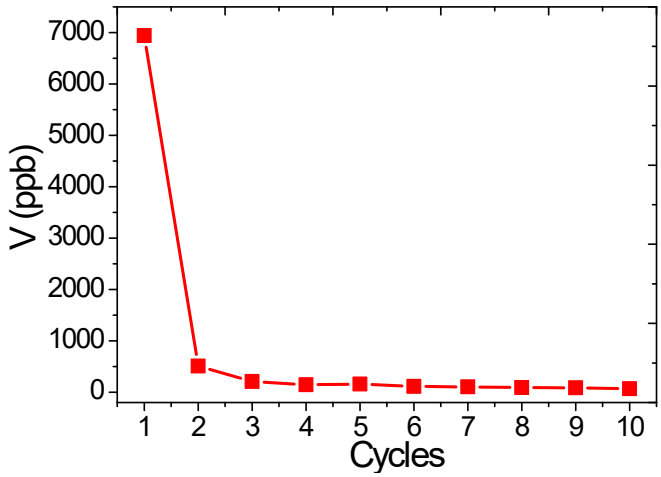

Figure S12 The V content in the electrolyte monitored by ICP-MS during the cycling test.

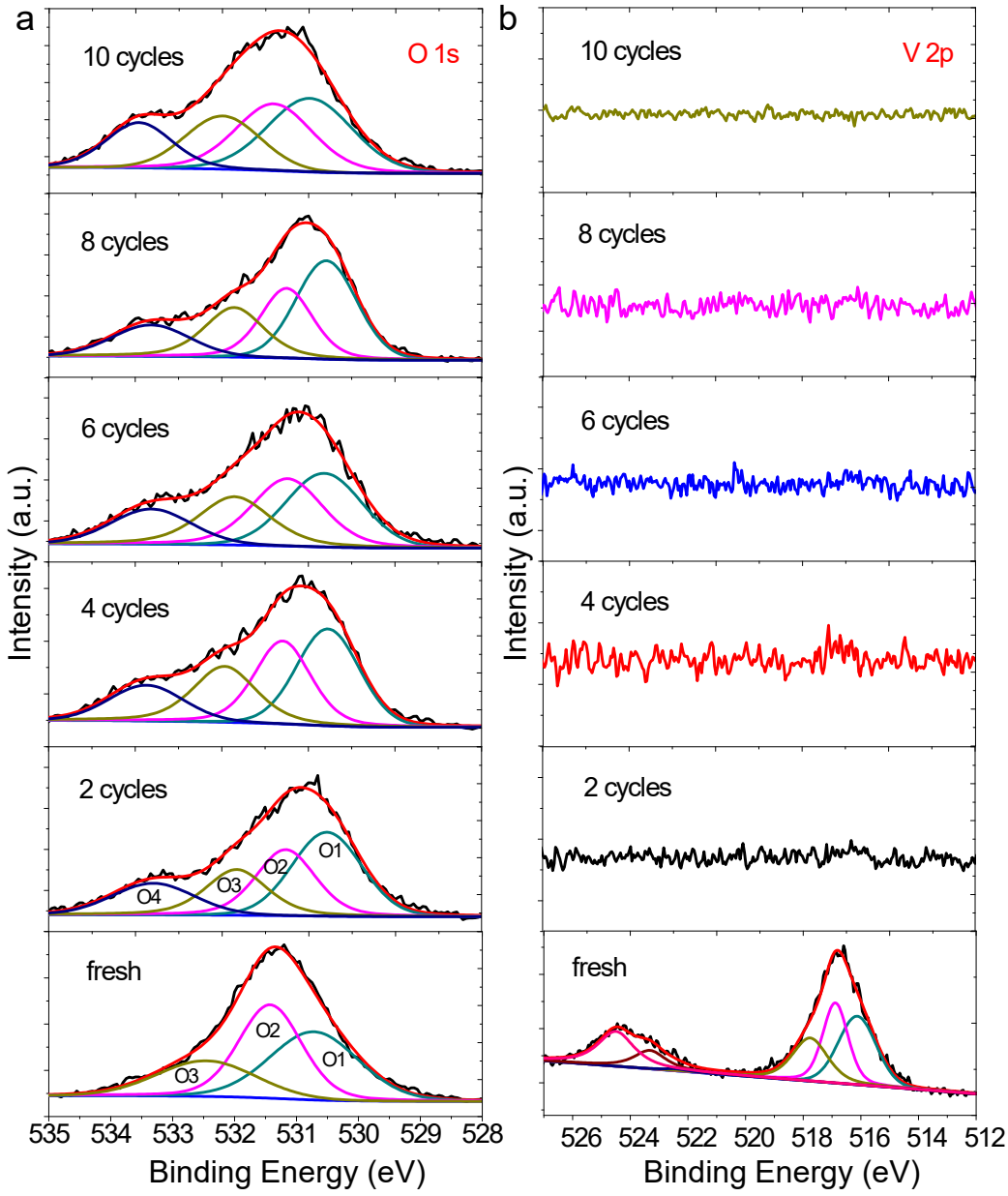

Figure S13 XPS spectrum of the (a) O 1s and (b) V 2p of NiVCo-LDHs during the cycling tests.

References

1. Song, Y.; Li, Z.; Fan, K.; Ren, Z.; Xie, W.; Yang, Y.; Shao, M.; Wei, M. Ultrathin layered double hydroxides nanosheets array towards efficient electrooxidation of 5-hydroxymethylfurfural coupled with hydrogen generation. *Appl. Catal. B* **2021,** *299,* 120669.

2. Qi, Y.-F.; Wang, K.-Y.; Sun, Y.; Wang, J.; Wang, C. Engineering the Electronic Structure of NiFe Layered Double Hydroxide Nanosheet Array by Implanting Cationic Vacancies for Efficient

Electrochemical Conversion of 5-Hydroxymethylfurfural to 2,5-Furandicarboxylic Acid. *ACS Sustain. Chem. Eng.* **2021,** *10*, 645-654.

3. Liu, B.; Xu, S.; Zhang, M.; Li, X.; Decarolis, D.; Liu, Y.; Wang, Y.; Gibson, E. K.; Catlow, C. R. A.; Yan, K. Electrochemical upgrading of biomass-derived 5-hydroxymethylfurfural and furfural over oxygen vacancy-rich NiCoMn-layered double hydroxides nanosheets. *Green Chem.* **2021,** *23*, 4034-4043.

4. Zhang, M.; Liu, Y.; Liu, B.; Chen, Z.; Xu, H.; Yan, K. Trimetallic NiCoFe-Layered Double Hydroxides Nanosheets Efficient for Oxygen Evolution and Highly Selective Oxidation of Biomass-Derived 5-Hydroxymethylfurfural. *ACS Catal.* **2020,** *10*, 5179-5189.

5. Zhang, J.; Yu, P.; Zeng, G.; Bao, F.; Yuan, Y.; Huang, H. Boosting HMF oxidation performance via decorating ultrathin nickel hydroxide nanosheets with amorphous copper hydroxide islands. *J. Mater. Chem. A* **2021,** *9*, 9685-9691.

6. Holzhäuser, F. J.; Janke, T.; Öztas, F.; Broicher, C.; Palkovits, R. Electrocatalytic Oxidation of 5-Hydroxymethylfurfural into the Monomer 2,5-Furandicarboxylic Acid using Mesostructured Nickel Oxide. *Adv. Sustain. Syst.* **2020,** *4* (10), 1900151.